Near-Infrared Light Is Neuroprotective in a Monkey Model of Parkinson Disease

Fannie Darlot, PhD,[1] Cécile Moro, PhD,[1] Nabil El Massri, BSc,[2] Claude Chabrol, PhD,[1] Daniel M. Johnstone, PhD,[3] Florian Reinhart, BSc,[1] Diane Agay, BSc,[1] Napoleon Torres, MD, PhD,[1] Dhaïf Bekha, BEng,[1] Vincent Auboiroux, PhD,[1] Thomas Costecalde, PhD,[1] Cassandra L. Peoples, BSc,[2] Helena D. T. Anastascio, BSc,[2] Victoria E. Shaw, MBBS, PhD,[2] Jonathan Stone, PhD, DSc,[3] John Mitrofanis, PhD,[2] and Alim-Louis Benabid, MD,PhD[1]

Objective: To examine whether near-infrared light (NIr) treatment reduces clinical signs and/or offers neuroprotection in a subacute 1-methyl-4-phenyl-1,2,3,6-tetrahydropyridine (MPTP) monkey model of Parkinson disease.
Methods: We implanted an optical fiber device that delivered NIr (670nm) to the midbrain of macaque monkeys, close to the substantia nigra of both sides. MPTP injections (1.5–2.1mg/kg) were made over a 5- to 7-day period, during which time the NIr device was turned on. This was then followed by a 3-week survival period. Monkeys were evaluated clinically (eg, posture, bradykinesia) and behaviorally (open field test), and their brains were processed for immunohistochemistry and stereology.
Results: All monkeys in the MPTP group developed severe clinical and behavioral impairment (mean clinical scores = 21–34; n = 11). By contrast, the MPTP-NIr group developed much less clinical and behavioral impairment (n = 9); some monkeys developed moderate clinical signs (mean scores = 11–15; n = 3), whereas the majority—quite remarkably—developed few clinical signs (mean scores = 1–6; n = 6). The monkeys that developed moderate clinical signs had hematic fluid in their optical fibers at postmortem, presumably limiting NIr exposure and overall clinical improvement. NIr was not toxic to brain tissue and offered neuroprotection to dopaminergic cells and their terminations against MPTP insult, particularly in animals that developed few clinical signs.
Interpretation: Our findings indicate NIr to be an effective therapeutic agent in a primate model of the disease and create the template for translation into clinical trials.

ANN NEUROL 2016;79:59–75

Parkinson disease (PD) is a movement disorder with cardinal signs of resting tremor, bradykinesia, and lead-pipe rigidity.[1–7] These manifest after a progressive death of many dopaminergic cells in the midbrain substantia nigra pars compacta (SNc) and the subsequent loss of their terminations in the striatum.[1–3,8] Unfortunately, the progression of this cell death has proved difficult to slow and impossible to reverse. The current treatment option for most patients is dopamine replacement drug therapy, which can be associated with, or followed by, surgery for deep brain stimulation (DBS).[9,10] Both of these treatments provide symptomatic relief—that is, they treat the signs that characterize the disease—but there is little evidence, at least in humans, for neuroprotection, a stopping of the underlying degeneration.[4–7] Hence, there is a real need to develop neuroprotective approaches that help slow this neurodegeneration.

Recently, it has been shown that near-infrared light (NIr) offers neuroprotection for various degenerative conditions, including PD.[11–13] NIr treatment has been reported to reduce cell death, increase adenosine

View this article online at wileyonlinelibrary.com. DOI: 10.1002/ana.24542

Received Jul 24, 2015, and in revised form Oct 7, 2015. Accepted for publication Oct 8, 2015.

Address correspondence to Dr Mitrofanis, Anderson-Stuart Building F13, Sydney, New South Wales, Australia. E-mail: john.mitrofanis@sydney.edu.au

From the [1]University Grenoble Alpes, CEA, LETI, CLINATEC, MINATEC Campus, Grenoble, France; and Departments of [2]Anatomy and [3]Physiology, University of Sydney, Sydney, New South Wales, Australia.

triphosphate (ATP) content, and decrease levels of oxidative stress among cultured cells after exposure to parkinsonian toxins.[12,14–16] Furthermore, NIr offers neuroprotection to dopaminergic cells in the well-known 1-methyl-4-phenyl-1,2,3,6-tetrahydropyridine (MPTP) mouse model[17–24] and in the K369I transgenic mouse model, which also shows a progressive degeneration of nigral dopaminergic cells.[25] Together with preserving dopaminergic cell survival in these models, NIr corrects the abnormal neuronal activity generated by MPTP toxicity,[26] as well as improving locomotor activity.[20,22,27]

It is not known whether NIr is, or can be, neuroprotective in humans. One potential problem with NIr delivered transcranially is the penetration of light energy over a large distance (80–100mm), from outside the skull to the deep regions of the brain and SNc.[13] It has been estimated that NIr may traverse a maximum of ~30mm through body tissues.[13] Thus, in humans, the quantity of transcranially delivered NIr energy reaching the SNc would be extremely low, perhaps undetectable.[13] To this end, we have been developing, based on our previous experience with endoventricular stimulation for obesity,[28] an intracranial optical fiber device for minimally invasive delivery of NIr in regions near the SNc, to ensure that stressed cells receive sufficient signal.[19,23]

In this study, we provide evidence that NIr is an effective therapeutic agent in a nonhuman primate model of PD. Our results showed that, when delivered by our newly developed intracranial optical fiber device, NIr had a striking impact on the behavior of MPTP-treated monkeys; the monkeys that received NIr exposure had less clinical impairment and more surviving dopaminergic cells than those that did not. These novel findings lay the essential template for translation into clinical trial.

Subjects and Methods

Subjects

Adult male macaque monkeys (*Macaca fascicularis*; n = 25) aged 4 to 5 years, weighing 5 to 7kg, were used. In accordance with animal welfare guidelines, animals were maintained in cages (2 per cage) under controlled conditions of temperature (25°C) and light (12-hour light/dark cycle); were fed regularly on a diet of fruit, vegetables, and pellets; and had free access to water. All experiments were approved by the Animal Ethics Committee COMETH (Grenoble) and the French Ministry for Research (protocol number 02790.01) and were performed in accordance with the European Communities Council Directive of 1986 (86/609/EEC) for care of laboratory animals. All participants of the team had received proper training and certification for animal experimentation. The conditions required by toxicology and security regulations were used throughout the period of MPTP injection and subsequent elimination from the animals.

Experimental Design

We used a subacute MPTP model that allows for toxic insult followed by a survival period sufficient for therapeutic intervention.[29,30] Within the timeline of the model, we used 2 MPTP dose regimes (1.5 and 2.1mg/kg) with 2 NIr doses (25 and 35J). The main experimental groups were (Fig 1):

1. Control (n = 5): none of these monkeys received MPTP treatment. Three monkeys had an optical fiber implant (but not activated) into the midbrain (see below), whereas 2 were left intact. A control group exposed to NIr was not included, because we have published previously that NIr has no impact on the survival and function of cells in normal brains.[17–25] Given the consistency of these results, together with the rareness of primate tissue and the ethical considerations to reduce the number of primates used, we felt that the extra control group was redundant and not justified in our study.
2. MPTP (n = 11): monkeys were administered 1.5mg/kg MPTP over 5 days (n = 6) or 2.1mg/kg over 7 days (n = 5); 10 of these monkeys were left intact, and 1 had an optical fiber implant (not activated).
3. MPTP-NIr (n = 9): monkeys were administered MPTP as above, in conjunction with optical fiber implants delivering NIr over 5 (total dose of 25J; n = 5) or 7 days (total dose of 35J; n = 4).

The NIr Optical Fiber Device

Based on our previous work in rodents,[19,23] we developed in-house a NIr laser optical fiber device linked to a pulse generator designed for monkeys (Boston Scientific, Natick, MA; Fig 2A–C). An optical fiber (HCP-MO200T) was attached to a small 670nm laser diode (optical power = 10mW). The optical fiber was plastic-coated, so as to limit leakage of NIr along the length of fiber and to focus on a small region (ie, the diffusor), ~3mm from the tip of the fiber. The proximal end of the device was connected through an extension lead to the rechargeable battery of an implantable stimulator (Boston Scientific Spectra), the same as those used for DBS, modified for our purposes by Boston Scientific. This was then used as a power generator. All devices were tested for power output using a calibrated light sensor (PM100D + S120VC; Thorlabs, Newton, NJ). The laser did not emit any measurable heat across the implant and SNc and was satisfactory for use over long periods.[22]

Surgical Procedure

Four weeks post-transportation, animals were anesthetized with ketamine (intramuscularly [im], 100mg/kg) and xylazine (im, 10mg/kg) and had 4.7T magnetic resonance imaging (MRI; Fig 3A, B) followed by ventriculography to determine target coordinates, as described previously.[28,29] Seven days later, the NIr optical fiber device was implanted stereotactically.[19,23] Animals were anesthetized as above, and the tissues overlying the cranium were reclined. Our aim was to implant stereotactically the optical fiber tip to a region 1 to 2mm to the left side of the midline in the midbrain, leaving the focal point of NIr intensity (~3mm

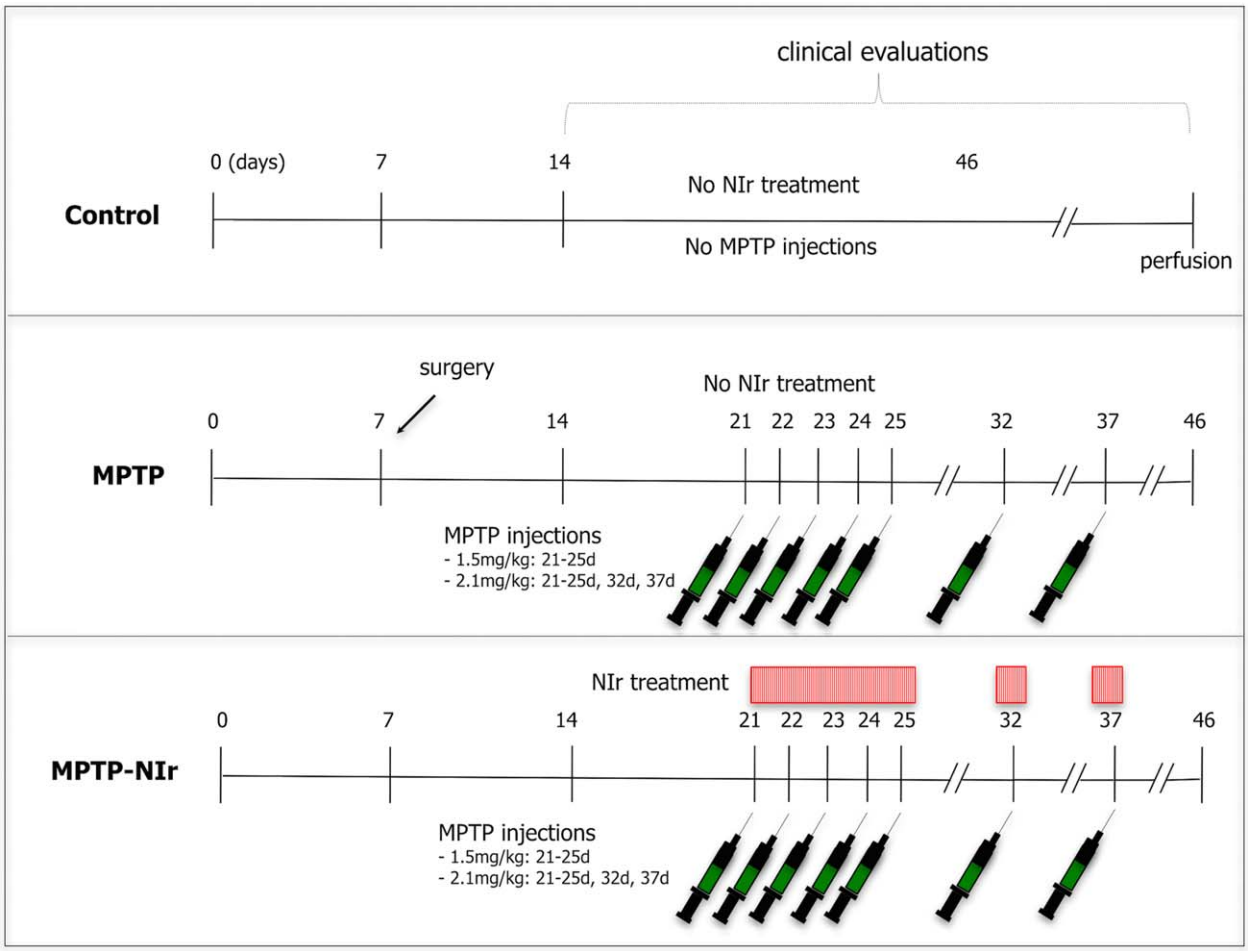

FIGURE 1: Outline of the experimental design of this study. We had 3 main experimental groups. The control group had no near-infrared light (NIr) treatment nor 1-methyl-4-phenyl-1,2,3,6-tetrahydropyridine (MPTP) injections. The MPTP group either had either a lower dose of 1.5mg/kg MPTP administered over 5 days (days 21–25; major period of MPTP injections) or a higher dose of 2.1mg/kg MPTP administered over 7 days (days 21–25, 32, 37). The MPTP-NIr group had the same MPTP dose regimes, together with 2 NIr dosages (25 or 35J; 5 seconds ON/60 seconds OFF over the 24-hour period after each MPTP injection). The MPTP-NIr monkeys had a magnetic resonance imaging scan and ventriculography to determine target coordinates after their postarrival recovery (day 0). A week later (day 7), monkeys had optical fibers implanted surgically into the midbrain, and MPTP injections were administered 2 weeks thereafter (day 21). The clinical evaluation of each monkey started 1 week after surgery (day 14). At the end of the experimental period, monkeys were perfused transcardially and processed for immunohistochemistry (day 46). It should be noted that 1 monkey from the MPTP group and 3 monkeys from the control

proximal to fiber tip) on the midline itself (see Fig 2). The approach was from the right side in an oblique trajectory; the implant site (4mm rostral to posterior commissure [PC], 3mm below anterior commissure [AC]–PC line, at the midline) was chosen because it was near the SNc, and in a position to provide equal amounts of NIr to the nucleus of both sides. The optical fiber positioning was cross-checked using measurements from intraoperative x-rays. After implantation, surgical dental cement (CMW1) was used to fill the skull opening, the laser device was fixed to the skull, and the stimulator and leads were placed in a subcutaneous pouch in-between the 2 shoulders. The overlying tissues were sutured, and antibiotic (im, Potencil; Virbac, Carros, France; 0.1ml/kg) and anti-inflammatory solutions (im, Kétofen 1%; Mérial, Lyon, France; 0.2ml/kg) were injected. All implants were tested after surgery for efficacy (arrows in Fig 2D, E). Animals were then allowed to recover for 14 days, during which time the device remained off. During the recovery, animals received antibiotic (for 5 days) and anti-inflammatory solution (for 3 days) as described above.

MPTP and NIr Treatments

Although there is no perfect model for idiopathic PD in humans, the monkey MPTP model is the most relevant available. This model has been shown to reproduce many of the patterns of dysfunction and degeneration of the dopaminergic system seen in idiopathic PD, together with a wide range of clinical signs, for example, bradykinesia and masklike facial expressions.[29–35] In this study, we used a subacute MPTP model that we have used previously.[29,33] Fourteen days postsurgery, a subset of animals (n = 6) received MPTP injections (im, 0.3mg/kg/day; Sigma, St Louis, MO) for 5 consecutive days (total of 1.5mg/kg) and were allowed to survive for 21

days after the last injection (see Fig 1). Other animals (n = 5) received 2 additional injections during the survival period (total of 2.1mg/kg), approximately 7 (±1) days apart. We hence explored the impact on cell loss and behavior after a lower and higher MPTP dose regime within our subacute model.

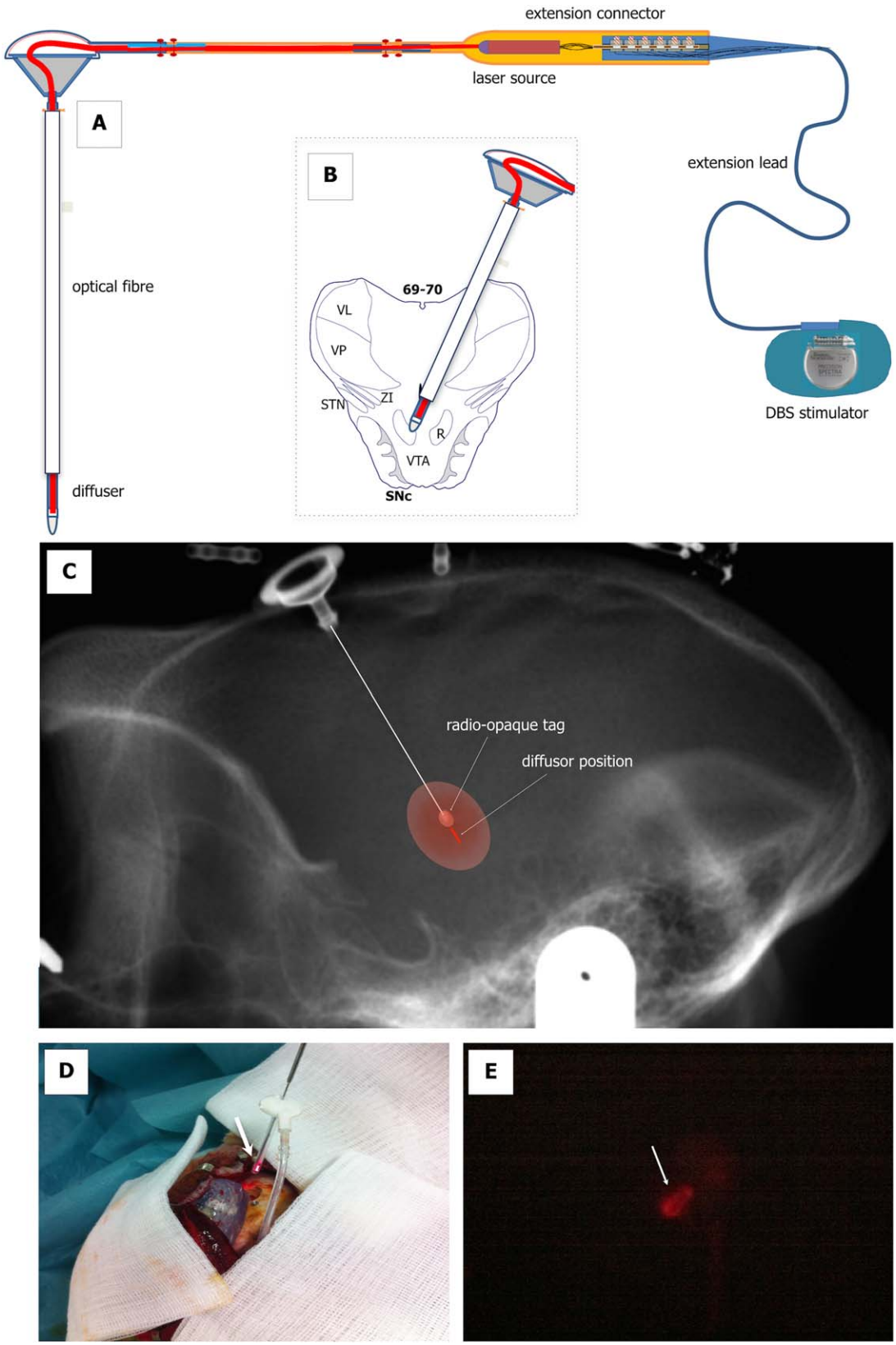

FIGURE 2.

For the NIr treatment, monkeys had the NIr device turned on (5 seconds ON/60 seconds OFF) a few minutes before each MPTP injection; the device remained turned on for the next 24-hour period (see Fig 1). The estimated total dose was either 25J for the monkeys receiving 1.5mg/kg MPTP over 5 days (n = 5) or 35J for the monkeys receiving 2.1mg/kg MPTP over 7 days (n = 4). Twenty-four hours after the last MPTP injection, the device was turned off. The paradigm of NIr treatment was designed to fit the electrical power of the Boston Scientific Spectra deep brain stimulation generator to the characteristics of the laser source and the needs of the experiment in energy delivered and in duration of the experiments.

During the experimental period, the function of the NIr device was checked, usually every few days after the device was turned on, with the aid of an ultrasensitive camera (PCO 1600; PCO, Kelheim, Germany); for this, the camera was directed toward the anesthetized (with ketamine/xylazine as described above) monkey's open mouth (see Fig 3C, D), and the NIr illumination (red glow) was verified across the palate and over the cranium (red arrows in Fig 3D). In addition, the function of the NIr device was checked at the conclusion of the experiment, just prior to perfusion (see below). If the device did not emit NIr, then these animals were excluded from the analysis (n = 4); in these cases, we could not be sure how much NIr was delivered during the period. In the majority of cases, animals with optical fiber implants had final MRI scans of their implant sites, just prior to perfusion. Note that, rather than providing implants to all the monkeys in the control and MPTP groups, we provided only 4; 3 in the control and 1 in the MPTP group (these devices were never activated). We felt this number would give a clear indication that the surgery did not impact on behavior or cell survival, while offsetting the high cost of the implants and surgery associated with each monkey, together with the ethics of reducing surgical procedures on nonhuman primates.

We estimated the amount of NIr signal reaching the SNc from our optical fiber device by modeling, using a range of different software, the key surrounding brain structures, together with the source of illumination. For the brain structures (eg, ventricles and SNc), we used an unbiased standard macaque monkey MRI template[36] and ran a segmentation using iTK-SNAP software to extract the structures of interest (see Fig 3E).[37] Once the segmentation step was complete, we exported the surface model generated in ITK-SNAP and converted it into a volume model with SolidWorks software. Finally, we imported our 3-dimensional (3D) model directly into the optical design and simulation software LightTools. In LightTools, we could attribute the optical parameters to each structure we had generated; for example, SNc was assimilated as pure gray matter and cerebrospinal fluid as having the refractive index of water. All the coefficients used in our simulation were from those outlined previously (see Table).[38] For our model of the illumination source, we represented the source as a cylinder emitting diffuse light in all space (see Fig 3F); the tip of the source was placed at 8.2mm distance away from SNc. The wavelength of the illumination was fixed, a pure monochromatic spectra with no drift in wavelength. The LightTools program performed a Monte Carlo simulation of the radiative transfer equation that was used to describe the propagation of light in a diffuse medium such as biological tissue.

Our experimental paradigm of simultaneous administration of MPTP insult and therapeutic application was similar to that of previous studies on animal models of PD.[17–24,29] This paradigm is unlike clinical reality, where there is cell loss prior to therapeutic intervention. However, in our experimental study we hoped to determine the maximal effect of any neuroprotection by NIr.

Clinical Evaluation

Animals were evaluated clinically in their home cages 7 days postsurgery and 7 days before the first MPTP injection, to establish baseline. Clinical evaluation continued during the series of MPTP injections and NIr treatments (or not) and then into the survival period after these treatments (see Fig 1). Animals were scored once per day (at the same time in the morning), every day, over a 20-minute period, by the same investigator (F.D.). A modified J. S. Schneider scale[34] was applied, and a range of parameters were rated, for example, posture, equilibrium, general activity, tremor, facial expression, bradykinesia, appetite, eye movements, and frequency of arm and leg movements. Each activity was scored from 0 to 3, with a total minimum score being 0 and maximum score achievable being 66. These scores were totaled for each day and are presented in Figure 4A. A mean clinical score for each group was calculated also; these mean values relate to the surface under the curve[35] and reflect the mean scores of monkeys throughout the experimental period. In addition to the changes in clinical score, that is, those related

FIGURE 2: (A) Schematic of our near-infrared light (NIr) laser optical fiber device linked to a pulse stimulator (Spectra, Boston Scientific). An optical fiber was attached to a small 670nm laser, which was connected through an extension lead to an implantable stimulator, the same as those used for deep brain stimulation (DBS). (B) Schematic diagram of a midbrain section indicating our target midbrain location, in-between the substantia nigra pars compacta (SNc) of both sides. (C) Sagittal X-ray of a monkey's head (within stereotaxic frame) with optical fiber device within midbrain; the optical fiber in this image is outlined by a white line. The radio-opaque tag is indicated, as is the diffusor position (and NIr halo). The positioning of the fiber was cross-checked using anterior commissure–posterior commissure distances and laterality from the midline measured from such X-rays. (D, E) Images of the optical fiber device being tested, just prior to (D) and after (E) implantation in the brain. The NIr was visible through the biological cement (*arrow* in E). The arrow in D indicates the focus of NIr near the distal end of the optical fiber. After this testing, the NIr was switched off, up until the injection period 2 weeks later. R = red nucleus; STN = subthalamic nucleus; VL = ventral lateral nucleus; VP = ventral posterior nucleus; VTA = ventral tegmental area; ZI = zona incerta.

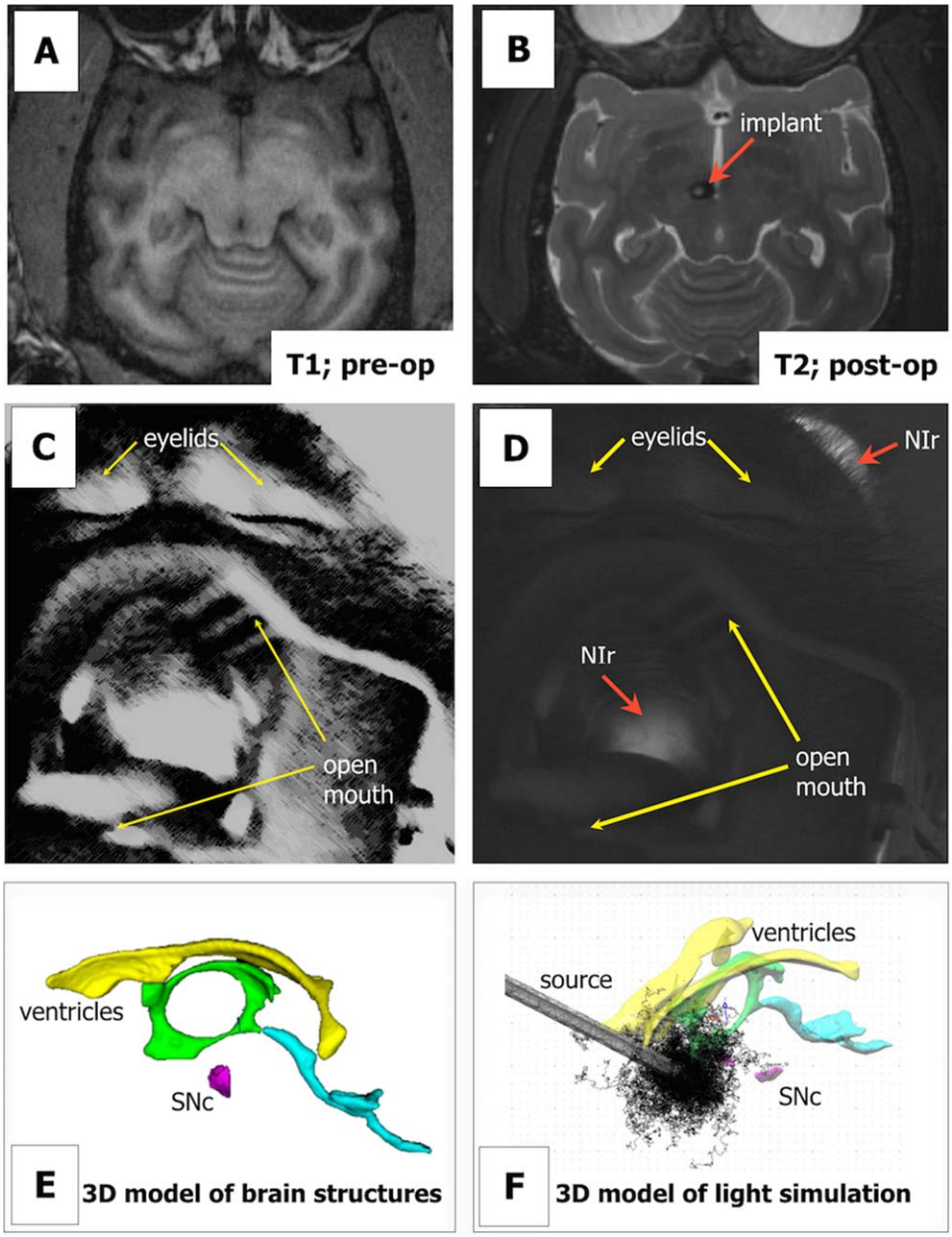

FIGURE 3: (A, B) Magnetic resonance imaging 4.7T images of monkey brain; A shows a T1-weighted image before surgery, whereas (B) shows a T2-weighted image of the same region after surgery (postoperative, scanned just prior to perfusion, ~40 days postsurgery). There is a signal area depicting the optical fiber within the midbrain, near the third ventricle (*arrow* in B). This monkey received a 35J near-infrared light (NIr) dosage, and there were no signs of a major inflammatory response surrounding the optical fiber. (C, D) Same frontal view of an anesthetized monkey's head; the eyelids and open mouth (with retractors) are indicated by yellow arrows. During the course of the experimental period, the function of the NIr device was checked using an ultrasensitive camera; the NIr illumination was verified across the palate and over the cranium (*red arrows* in D). The function of NIr device was checked also at the conclusion of the experimental period, just prior to perfusion. (E, F) Three-dimensional (3D) models of key brain structures and simulation of light dissipation from the source, using a range of software (see Subjects and Methods for details). SNc = substantia nigra pars compacta.

to the effect of MPTP insult and NIr treatment, we also noted the clinical signs evident in the immediate postoperative period that were related to the surgical implantation of the optical fiber, for example, to the internal capsule (hemiparetic deficits), the oculomotor (third) nerve (mydriasis), and to the trochlear (fourth) nerve (gaze deviations). For comparisons of mean clinical scores between 3 or more groups, a 1-way analysis of variance (ANOVA) test was performed, in conjunction with a post hoc Tukey–Kramer multiple comparison test; for comparisons of mean scores between 2 groups, a standard *t* test (unpaired, 2-tailed) was used (Prism; GraphPad, San Diego, CA).

It should be noted that the monkeys in the MPTP group that developed severe clinical signs after MPTP injection (see Results) were not readily able to eat and drink autonomously. Hence, these monkeys received, when appropriate, apomorphine (10mg/ml subcutaneously; Apokinon; Laboratoire Aguettant, Saint-Fons, France) and/or oral administration of L-dopa (10–100mg Sinemet [L-dopa–carbidopa]; MSD, Courbevoie, France). The doses of the agents were adjusted to the health status of the animal; the treatment allowed the animal to recover its ability to feed itself and move. This was undertaken in the late morning after all behavioral tests were complete and, if required, in the afternoon as well. This process ensured enough time for the drug to be cleared from the monkey's system by the next morning's testing. These animals also received a high-calorie diet supplement.

Behavioral Activity

In addition to the clinical evaluation, we examined the behavioral locomotor activity of monkeys in the different groups in their home cages using an open field test. For this, activity was videotaped using a high-definition camera linked to the Noldus program (EthoVision, XT 10 version; Noldus, Wageningen, the Netherlands) that detected the movement of the monkeys in their cages. Animals were fitted with different colored jackets, and the program was set to detect the movement of the jacket. The movements were recorded over a 20-minute period on each day during the entire experimental period, from baseline to the last day of testing. The program then recorded a trace pattern of movement, as well as quantifying the total distance moved and maximal velocity of movement (Vmax) during the 20-minute period (see Fig 4). For quantification, the percentage change in distance moved and Vmax from the average baseline values (100%) to the average values attained during the last 5 days of testing (the period of peak change) was calculated for each monkey. The results are presented for the MPTP and MPTP-NIr groups; the control group had no change in activity during this period and hence a value of 0. For comparisons in locomotor activity between groups, we used ANOVA and Tukey–Kramer tests (see above).

Immunohistochemistry and Cell Analysis

At the end of the experimental period, animals were anesthetized with sodium pentobarbital (im, 60mg/kg). They were then perfused transcardially with a clearing solution (NaCl 0.9%, sucrose 0.8%, glucose 0.4%) followed by 4% buffered paraformaldehyde (Sigma). The brains were removed and post-fixed overnight in the same solution. Next, brains were placed in phosphate-buffered saline (PBS) with the addition of 30% sucrose until the block sank. The forebrain was then sectioned coronally and serially using a freezing microtome. All sections were collected in PBS and then immersed in a solution of PBS and 10% normal mouse serum (M5905, Sigma) and then PBS and 1% Triton (X100, Sigma) each for ~1 hour at room temperature. Sections were then incubated in either anti–tyrosine hydroxylase (TH; 1:500; T8700, Sigma; to label dopaminergic cells in SNc), anti-glial fibrillary acidic protein (GFAP; 1:500; Z033429-2; Dako, Glostrup, Denmark; to label astrocytes adjacent to implant site), or anti–ionized calcium binding adaptor molecule 1 (IBA1; 1:500; 019-19741; Wako Chemicals, Richmond, VA; to label microglia adjacent to implant site) for 48 hours (at 4°C), followed by biotinylated antirabbit immunoglobulin G for 4 hours and then ExtrAvidin–peroxidase complex for 2 hours (both at room temperature; 1:20, EXTRA3-1KT, Sigma). To visualize the bound antibody, sections were reacted in a 3,3′-diaminobenzidine tetrahydrochloride solution (D3939, Sigma). Sections were mounted onto gelatinized slides, air dried overnight, dehydrated in ascending alcohols, cleared in Histoclear, and coverslipped using Depex (DPX). As a rule, forebrain (including striatum) was immunostained for TH; midbrain (including the implant sites) was Nissl-stained (with cresyl violet or neutral red; to label all cells adjacent to implant site and within SNc) and immunostained for TH, GFAP, or IBA1. For controls, sections were processed as described above except that no primary antibody was used. These control sections were immunonegative.

TABLE. Coefficients of Tissues Used to Calculate Near-Infrared Light Levels in Substantia Nigra Pars Compacta

Coefficient	Gray Matter	White Matter
μ_a, per mm	0.02	0.07
μ_s, per mm	8.4	40.1
g	0.9	0.85
n	1.36	1.38

Values taken from Yaroslavsky et al.[38]

Nigral cells were identified by TH immunohistochemistry and Nissl staining. We used both these methods to determine whether changes in cell number after MPTP or NIr treatments were due to true cell survival or to a loss of functional capability, that is, a loss of antigen expression (TH). Nissl staining labels all cells regardless of phenotypic expression, whereas TH immunohistochemistry labels healthy cells that express the dopamine phenotype, hence providing an index of function of dopaminergic cells.[39–41] In essence, we explored whether there was true and/or functional neuroprotection. The number of nigral TH^+ and Nissl-stained cells (main body of the nucleus, ie, ventral tier)[8,29] was estimated using the optical fractionator method (Stereo Investigator; MBF Bioscience, Williston, VT), as outlined previously.[17–24,29] Briefly, systematic random sampling of sites—with an unbiased counting frame—within defined boundaries of SNc was undertaken. All cells that came into focus within the frame were counted, and at least 10 sites were sampled per section in the SNc. We also measured the density of TH^+ terminals in the striatum, the major site of termination of the nigral dopaminergic cells. Bright field images of striatal TH^+ terminals were captured under standard illumination conditions for each section. Each image was then

processed in an identical manner using ImageJ software (NIH, Bethesda, MD). For each image, color threshold was adjusted to a set level, when the TH^+ terminals were distinguished from background. The mean gray value was then measured for each image. The resulting values in the striatum provided a reliable and replicable measure of the density of TH^+ terminals in each image. We have shown previously that there is no evidence for a natural asymmetry in the number of nigral cells of

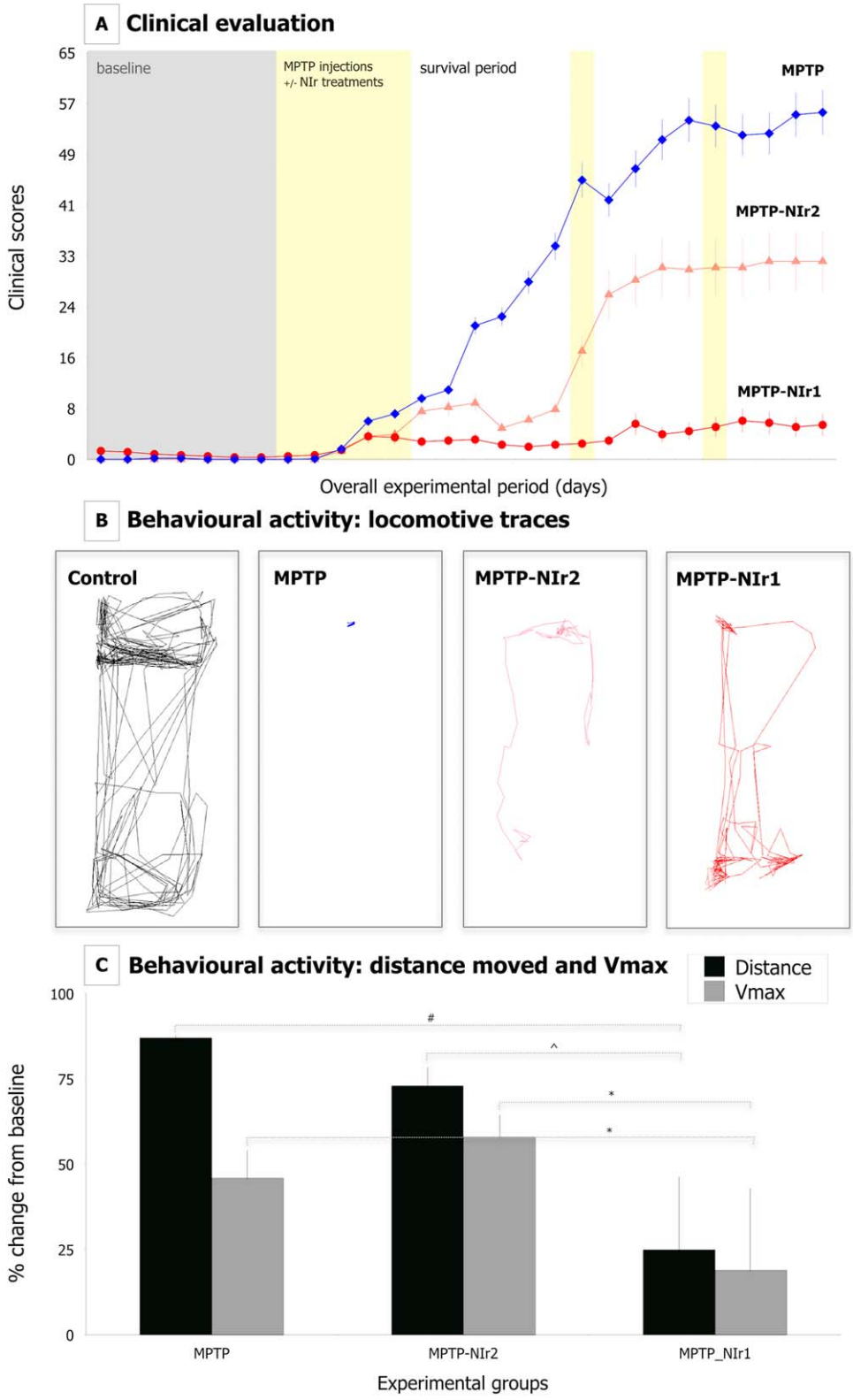

FIGURE 4.

monkeys.[29] Nevertheless, for the sake of consistency, our analysis of cell number and terminal density was undertaken on the right side (the side opposite from the implant site) of the brain in each case. We did however undertake bilateral counts of MPTP-NIr monkeys to explore the potential neuroprotective efficacy of NIr on the SNc of both sides, namely, whether there was any laterality of effect. We also measured the area of our implant sites in the midbrain using the Stereo Investigator program. The boundaries of the implant sites from immunostained sections were outlined, and the program calculated the area. For comparisons in SNc cell number and striatal terminal density between groups, we used ANOVA and Tukey–Kramer tests, whereas for a comparison between the implant site areas in NIr-treated and control–sham animals, a standard t test was used (see above).

Correlation Coefficients

To explore the relationship between the extent of nigral and striatal lesion and mean clinical scores in individual monkeys, the correlation coefficients (Pearson test) were calculated (GraphPad Prism). The extent of nigral and striatal lesion for each monkey in the MPTP and MPTP-NIr groups was calculated as a percentage change of either nigral TH^+ cell number or striatal TH^+ terminal density from mean control values attained from the monkeys in the control group. The Pearson test generates a correlation factor (r value) that, if close to 1, indicates that the correlation is significant. A measure of goodness-of-fit of linear regression is r^2, and the closer the value is to 1, the better x (eg, extent of nigral or striatal lesion) predicts y (eg, mean clinical score).

Results

General Observations

No major adverse effects were observed following surgical implantation of the optical fiber, with monkeys resuming normal activity within a few hours postsurgery.[19,23] There was never any sign of distress caused by the NIr. On the contrary, the NIr-treated animals had a reduction in clinical impairment (see below). Under normal room lighting conditions, NIr was not evident externally after the device was turned on. When the lights were dimmed, however, the NIr was seen clearly through the biological cement surrounding the laser device during the last steps of the implantation (see Fig 2D).

Clinical Evaluation

The degree of clinical impairment was expressed by increasingly higher clinical scores (see Fig 4A). Clinical scores of the control group (both operated and intact) were 0 throughout the experimental period.[29] This was also true for most monkeys (operated and intact) during the baseline recordings (see Fig 4A). Thus, surgery and/or optical fiber implantation had no major impact on behavior.

For the MPTP group, there were no significant differences in clinical scores between the 1.5mg/kg or 2.1mg/kg MPTP dose regimes ($p = 0.8$). Hence, their data were pooled. For this group, clinical scores increased dramatically soon after the last MPTP injection, during the first few days of the survival period. They then stabilized, remaining consistently high up until the last day of testing (see Fig 4A). The mean clinical scores of the different monkeys in this group over the entire experimental period ranged from 21 to 34. The MPTP monkey that had an optical fiber implant (and the device not turned on) achieved clinical scores within the range of the intact MPTP monkeys, strengthening further the notion that the surgery and/or optical fiber implants had no impact on behavior (see above). It should be noted that, for some autonomous activity and for eating and drinking, all of the MPTP group received apomorphine or L-dopa treatment immediately after behavior testing.

For the MPTP-NIr group, all animals had less clinical impairment than those in the MPTP group and

FIGURE 4: (A) Graphs of the clinical scores of monkeys in the 1-methyl-4-phenyl-1,2,3,6-tetrahydropyridine (MPTP) and MPTP–near-infrared light (NIr) groups. Two groups of MPTP-NIr monkeys were distinguished: MPTP-NIr1 (with minimal clinical signs) and MPTP-NIr2 (with moderate clinical signs). Both the MPTP-NIr groups had clinical scores much lower than the MPTP group. Markers show the mean ± standard error of the total number in each group. The graphs show the clinical scores from the baseline period (gray shading), the main period of MPTP injections and NIr treatments (or not; thick band of yellow shading), the 2 extra MPTP injections and NIr treatments (thin strips of yellow shading; in the higher dose regime), and the survival period after treatments. The clinical scores of the monkeys in the control group was 0 (see also Wallace et al[29]. (B) Examples of the behavioral locomotive activity of individual monkeys in the control, MPTP, and MPTP-NIr1 groups using an open field test. Each figure in B shows a trace, generated by the Noldus program (Ethovision, XT 10 version), outlining the movement of an individual monkey in its home cage over a 20-minute period. For the MPTP and MPTP-NIr1 monkeys, traces were taken during the main period of MPTP injections. During the 20-minute period of recording, the traces indicated that the monkey in the MPTP group (blue trace) had much less movement around its home cage than the control monkey (black trace); the monkey in the MPTP-NIr1 group (red trace), although less active than the control monkey, had considerably more activity than the monkey in the MPTP group. The monkey in the MPTP-NIr2 group (light red trace) had more active tracers than the MPTP group but fewer than the MPTP-NIr1 group. (C) Quantification of behavioral locomotive activity from open field test. The percentage change in distance moved (black columns) and Vmax (maximal speed; gray columns) from the average baseline values (100%) to the average values attained during the last 5 days of testing (the period of peak change) was calculated for each monkey. The results are presented for the MPTP, MPTP-NIr1, and MPTP-NIr2 groups; the control group had no change in activity during this period and hence a value of 0.

none required apomorphine or L-dopa treatment. There was some variation in the mean clinical scores of the MPTP-NIr group; it was clear that some of these monkeys developed many fewer clinical signs than others. We could distinguish 2 subgroups of MPTP-NIr monkeys

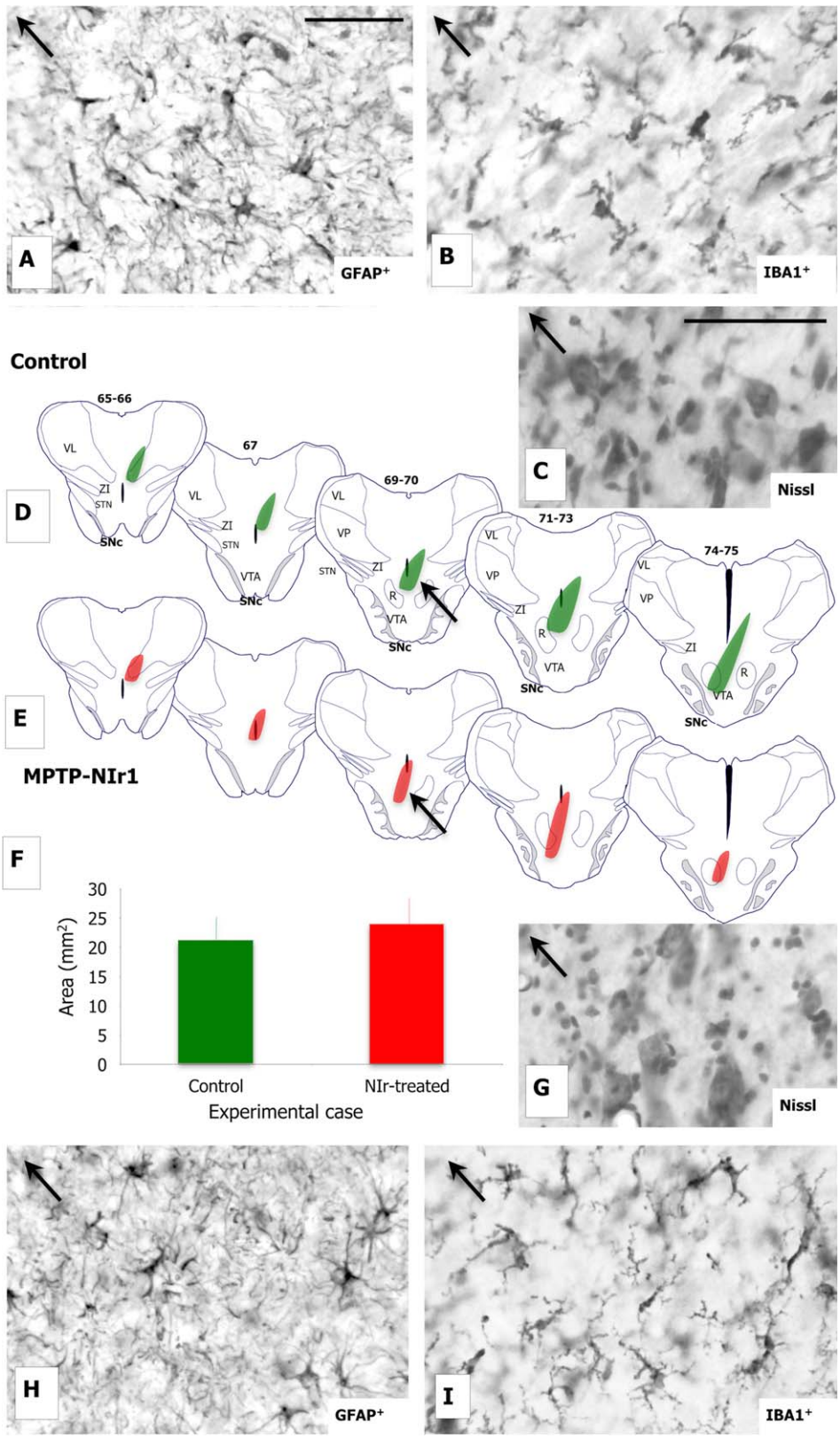

FIGURE 5.

(see Fig 4A); these 2 subgroups were made up of animals from both MPTP dose regimes.

The MPTP-NIr1 group (n = 6) had, quite strikingly, virtually no clinical signs. Their clinical scores did not increase dramatically soon after the period of MPTP injections; rather, these monkeys had a very small increase in scores that, over the ensuing period, did not change up to the last day of testing (see Fig 4A). The mean clinical scores of the different monkeys in this group ranged from 1 to 6, ~90% lower than the MPTP group ($p < 0.00001$). Three of these monkeys were from the lower MPTP dose regime and 3 from the higher one.

The MPTP-NIr2 group (n = 3) developed moderate clinical signs. Their clinical scores increased slightly after the main period of MPTP injections but then stabilized, not changing up until the last day of testing. The mean clinical scores of the different monkeys in this group ranged from 11 to 15, ~50% lower than the MPTP group ($p < 0.001$). Two of these monkeys were from the lower MPTP dose regime and 1 from the higher one. For this group, the catheter bearing the optical fiber, including the NIr diffusor part of the probe, was found filled with hematic fluid at postmortem. By contrast, none of the MPTP-Nr1 group had fluid in the catheter. This feature may have reduced NIr exposure to the SNc and led to the differences in clinical scores evident between the MPTP-NIr groups.

Overall, the differences in clinical scores between the MPTP, MPTP-NIr1, and MPTP-NIr2 groups were significant ($p < 0.0001$). It should be noted that the variations in clinical scores of the MPTP-NIr group were in stark contrast to the MPTP group; without exception, each monkey in the MPTP group developed severe clinical signs, and no distinct subgroups were distinguished.

Behavioral Activity

Figure 4B and C show the results of the behavioral locomotor activity from our open field test. Figure 4B shows examples of traces of locomotor activity for individual monkeys in the different experimental groups. These traces highlight the features described above for the clinical evaluations. The MPTP-NIr1 group, although not quite as active as the control group, showed considerably more movement across the home cage than the MPTP group. The MPTP-NIr2 group had more active traces than the MPTP group but less than the MPTP-NIr1 group. Figure 4C quantifies the percentage change in distance moved and Vmax during the experimental period in the MPTP, MPTP-NIr1, and MPTP-NIr2 groups (the control group had no change in activity and hence a score of 0). The MPTP and MPTP-NIr2 groups had the largest percentage change in both parameters, reflecting their lower levels of mobility. They had approximately the same Vmax, but the MPTP group had a larger reduction in distance moved. Notwithstanding, the differences between the 2 groups were not significant ($p > 0.05$). The MPTP-NIr1 group had the smallest percentage change, reflective of their greater mobility; the differences between this group and the others for both distance moved and Vmax were significant.

Optical Fiber Implant Sites in Midbrain

All our implant sites were found close to the midline in the midbrain, traversing the third ventricle and often encompassing the ventral tegmental area and red nucleus (Fig 5D, E); the tip of the optical fiber was usually 1 to 2mm to the left of the midline, with the focal point of NIr intensity being very near the midline itself, equidistant from the SNc of both hemispheres.

In general, we found no major effect of NIr around the implant site. Control and MPTP-NIr showed similar labeling patterns with Nissl staining (labeling all cells), GFAP immunostaining (labeling astrocytes), and IBA1 immunostaining (labeling microglia; see Fig 5). No NIr-treated case showed zones of necrosis or gliosis surrounding the optical fiber implant site. Any cellular damage appeared mechanical, due to tissue displacement by the fiber and/or tip; control and NIr-treated cases showed

FIGURE 5: Schematic diagrams and photomicrographs of our optical fiber implant sites in a control case (no near-infrared light [NIr]; A-D) and a 1-methyl-4-phenyl-1,2,3,6-tetrahydropyridine (MPTP)–NIr1 case (E–I). Implant sites were found close to the midline in the midbrain, traversing the third ventricle and often encompassing the ventral tegmental area and red nucleus (D, E); the tip of the optical fiber was often 1 to 2mm to the left of the midline, with the focal point of NIr intensity being near the midline, equidistant from the substantia nigra pars compacta (SNc) of both sides. There were no differences in Nissl staining (C, G) nor glial fibrillary acidic protein (GFAP; A, H) and ionized calcium binding adaptor molecule 1 (IBA1) immunostaining (B, I) between the control and MPTP-NIr cases. There was no evidence of NIr toxicity. The only cellular damage evident appeared mechanical, being caused after tissue displacement by the fiber and/or tip itself. All figures are of coronal sections, dorsal to top, medial to left. Scale bar = 100μm; in A it applies also to B, H, and I; in C, the scale applies also to G. (F) Graph of the areas of the implant sites in the control case and our NIr-treated cases. Note that the areas of the control and NIr-treated implants were similar. Arrows indicate approximately the same region in the schematics and photomicrographs. R = red nucleus; STN = subthalamic nucleus; VL = ventral lateral nucleus; VP = ventral posterior nucleus; VTA = ventral tegmental area; ZI = zona incerta.

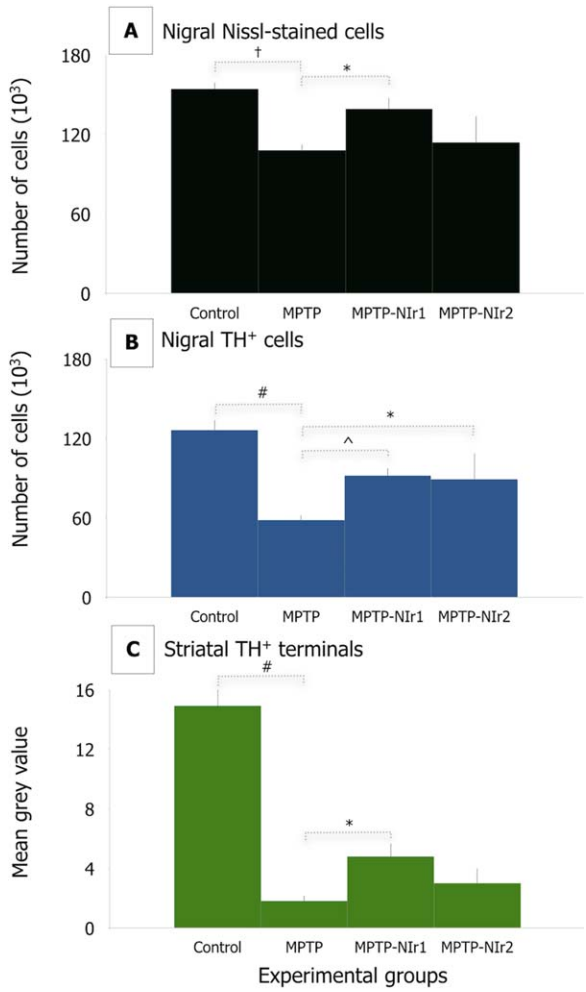

FIGURE 6: Graphs of the mean number of nigral Nissl-stained (A; black columns) and tyrosine hydroxylase (TH)$^+$ (B; blue columns) cells and mean density of striatal TH$^+$ terminals (C; green columns) of monkeys in the control, 1-methyl-4-phenyl-1,2,3,6-tetrahydropyridine (MPTP), and MPTP–near-infrared light (NIr; distinguished after clinical scoring) groups. The columns show the mean ± standard error in each group. The symbols indicate levels of significant difference between the MPTP and MPTP-NIr groups: #$p<0.00001$, †$p<0.0001$, ^$p<0.001$, *$p<0.05$.

comparable patterns of gliosis along the fiber tract through the forebrain and midbrain. The area of the implant site was very similar in NIr-treated and control cases ($p = 0.8$). Finally, MRI images before (see Fig 3A) and after surgery (see Fig 3B) revealed no evidence of a major inflammatory response surrounding the optical fiber (red arrow Fig 3B) within the midbrain.

With the use of 3D modeling and simulation software (see Subjects and Methods and Fig 3E, F), our estimation of the amount of energy absorbed by the SNc was 169nW. This indicated that from the source (10mW) to the SNc, there was <99% dissipation of power intensity. This value is consistent with previous estimates over similar distances of brain tissue.[19]

Number and Morphology of Nigral Dopaminergic Cells and Striatal Terminations

Figure 6 shows the number of nigral Nissl-stained and TH$^+$ cells and the density of striatal TH$^+$ terminals in the different groups. Two striking patterns were evident. First, the MPTP group, the monkeys that developed the most severe clinical impairment, had substantial reductions in the number of nigral Nissl-stained (~30%; $p < 0.0001$) and TH$^+$ (~50%; $p < 0.00001$) cells and density of striatal TH$^+$ terminals (~90%; $p < 0.00001$) compared to the control group. These findings indicated that our MPTP dose regimes were effective in generating cell loss; as with our behavioral analyses, we found no differences ($p > 0.05$) in nigral cell number and striatal terminal density between the 2 MPTP dose regimes, hence their data were pooled.

Second, the MPTP-NIr1 group, the monkeys that developed virtually no clinical impairment, had more nigral Nissl-stained (~20%; $p < 0.05$) and TH$^+$ (~40%; $p < 0.001$) cells and striatal TH$^+$ terminals (~60%; $p < 0.05$) than the MPTP group (see Fig 6). These values for the MPTP-NIr1 group were not quite up to control levels, however, particularly in striatal terminal density ($p < 0.00001$). Furthermore, the MPTP-NIr2 group, the monkeys that had more moderate clinical impairments, had values generally lower than those in the MPTP-NI1 group and, most notably, higher than in the MPTP group, particularly in the number of TH$^+$ cells ($p < 0.05$).

To determine if there was a laterality of the NIr treatment, we undertook bilateral counts of nigral TH$^+$ cells in the MPTP-NIr groups. These counts revealed no significant differences ($p = 0.9$) between the 2 hemispheres (left:right ratio = 1.02).

Figure 7 shows representative photomicrographs of nigral cells and their striatal terminations in the different groups. In the control group, the nigral cells had strong Nissl staining and TH immunoreactivity localized to their cytoplasm. In the striatum, TH immunoreactivity was seen in many fibers and numerous small terminals, forming a characteristic dark haze of immunoreactivity across the nucleus. In the MPTP group, the nigral cells tended to be smaller and had weaker Nissl staining. TH immunoreactivity was often quite intense in the surviving cells, and there were many small TH$^+$ structures scattered across the SNc, presumably remains of degenerated cells (arrows in Fig 7E). In the striatum of the MPTP group, the nucleus was largely barren of immunoreactivity, with only very few TH$^+$ terminals seen. In the MPTP-NIr1 group, the Nissl-stained and TH$^+$ cells of the SNc were more similar to the controls; Nissl staining was more robust, and there was less TH$^+$ debris in the

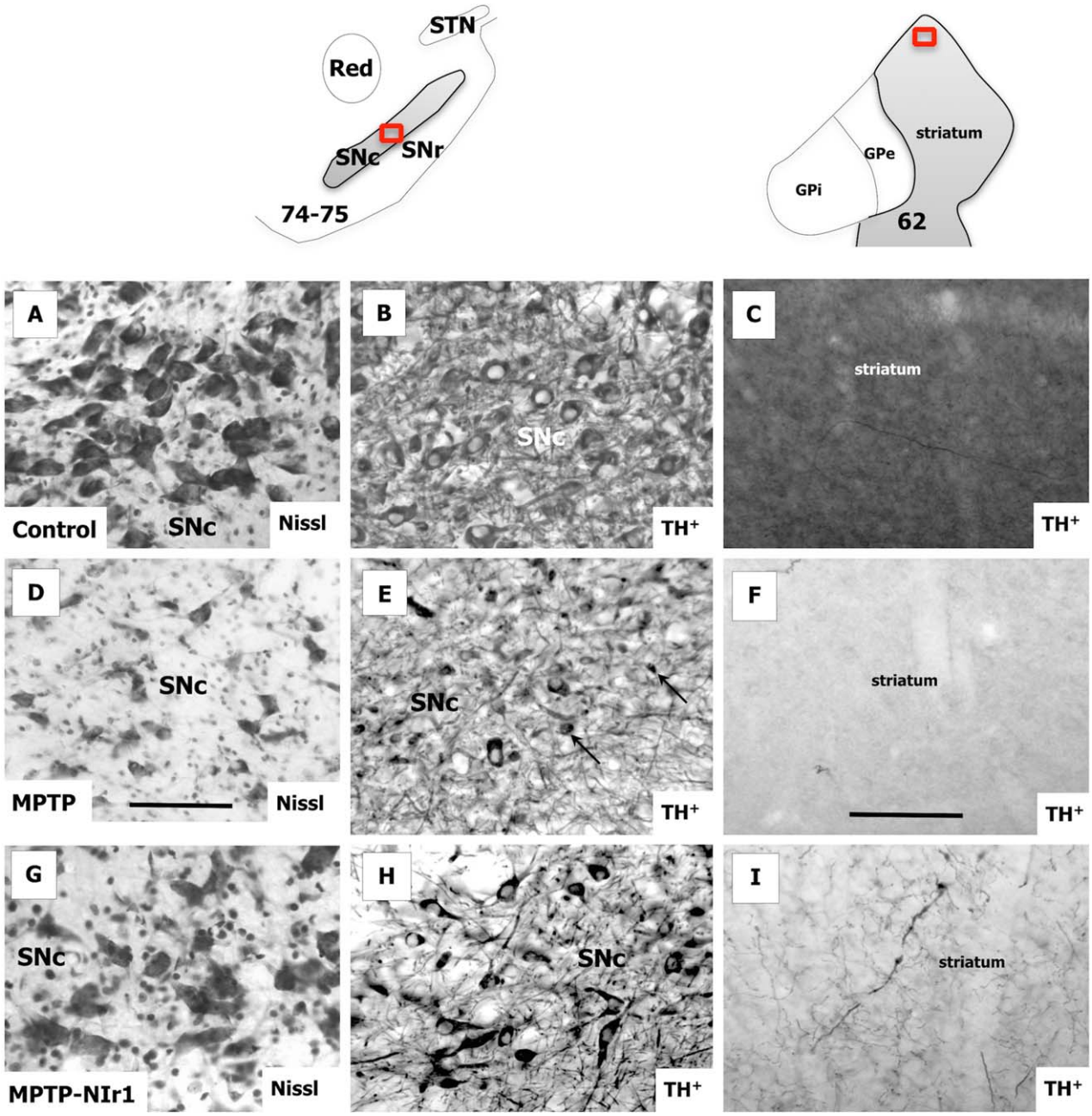

FIGURE 7: Photomicrographs of nigral Nissl-stained (A, D, G) and tyrosine hydroxylase (TH)$^+$ (B, E, H) cells and of striatal TH$^+$ terminations (C, F, I) in the control (A, B, C), 1-methyl-4-phenyl-1,2,3,6-tetrahydropyridine (MPTP; D, E, F) and MPTP–near-infrared light 1 (NIr1; G, H, I) groups. Images from the other MPTP-NIr groups were similar to the MPTP-NIr1 group, except that the numbers of nigral Nissl-stained cells and striatal terminations were lower (see Results). For the substantia nigra pars compacta (SNc), each photomicrograph was taken from a central region, in sections corresponding to plates 69 to 70 of a monkey atlas.[47] Arrows in E indicate small TH$^+$ structures, likely to be remains of degenerated cells. For the striatum, each photomicrograph was taken from a dorsal region, corresponding to plates 63 and 64 in the atlas.[47] All figures are of coronal sections, dorsal to top, medial to left. Scale = 100μm in D (relates to A, B, D, E, G, H) and in F (relates to C, F, I). GPe = globus pallidus externus; GPi = globus pallidus internus; SNr = substantia nigra pars reticulata; STN = subthalamic nucleus. [Color figure can be viewed in the online issue, which is available at www.annalsofneurology.org.]

SNc. In the striatum of the MPTP-NIr1 group, there were generally more TH$^+$ terminals than in the MPTP group, albeit many fewer than in the control group; although there was this increase in terminations, the dark haze of immunoreactivity evident in the controls was never seen in the MPTP-NIr1 group. These patterns of morphology in the SNc and striatum of the MPTP-NIr1 group were evident in the MPTP-NIr2 group also, except that the MPTP-NIr1 group had more nigral Nissl-stained cells and striatal TH$^+$ terminals (see above).

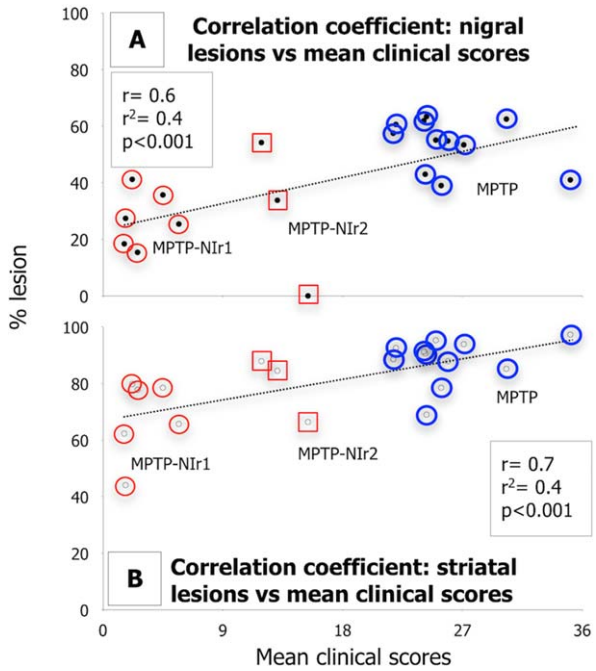

FIGURE 8: Correlation between the extent of nigral (A) and striatal (B) lesion and mean clinical scores in individual monkeys in the 1-methyl-4-phenyl-1,2,3,6-tetrahydropyridine (MPTP) and MPTP–near-infrared light (NIr) groups. The extent of nigral *(black circles)* or striatal *(white circles)* lesion for each monkey is expressed as a percentage change in tyrosine hydroxylase immunoreactivity from the controls. In general, monkeys with higher mean clinical scores tended to have larger lesions, namely the MPTP *(blue circles)* group. Monkeys with smaller lesions tended to have lower mean clinical scores; these formed the MPTP-NIr1 *(red circles)* and MPTP-NIr2 *(red squares)* groups. The correlations between nigral and striatal lesions and mean clinical scores were significant.

Correlation between Anatomical Lesion and Clinical Score

We next correlated the extent of nigral and striatal lesion with mean clinical score for each monkey (Fig 8). For the SNc and striatum, there was a tendency for monkeys with higher clinical scores to have larger lesions; the majority of these monkeys formed the MPTP group (blue circles). The monkeys with smaller nigral lesions were more likely to have lower clinical scores, and these monkeys formed the MPTP-NIr1 (red circles) and to lesser extent the MPTP-NIr2 (red squares) groups. There were some variations however, particularly in the MPTP-NIr2 group. For example, 1 of these monkeys showed no sign of nigral lesion (0), but had a mean clinical score of 15, whereas other monkeys had massive striatal lesions (85–90%), but had mean clinical scores of 11 to 13. Notwithstanding these variations, there was a significant correlation between nigral ($r = 0.6$, $r^2 = 0.4$; $p < 0.001$) and striatal ($r = 0.7$, $r^2 = 0.4$; $p < 0.001$) lesions and mean clinical scores.

Discussion

We showed that intracranially delivered NIr had a striking impact on the behavior of monkeys after MPTP insult; the MPTP-NIr group had reduced clinical impairment compared to those that were untreated. Furthermore, we showed that the NIr had no toxic effects on brain parenchyma and was neuroprotective to nigral dopaminergic cells and their striatal terminations, particularly in monkeys with the largest reductions in clinical signs.

NIr Reduced Clinical Impairment

The results were unequivocal. The intracranially delivered NIr was not only well tolerated by the monkeys, with none showing any visible signs of discomfort, but it reduced markedly their clinical scores after MPTP insult. During the course of the experimental period after the main period of MPTP injections, the mean clinical scores of the MPTP-NIr group were, albeit not quite at control levels, considerably less than those of the MPTP group. NIr not only offset the dramatic increase in clinical scores, but kept them lower right up until the last day of the experimental period. These findings are consistent with previous studies reporting that NIr improves locomotive behavior in MPTP-treated mice using an open field test[20,27] and reduces apomorphine-induced turning behavior in 6-hydroxydopamine–lesioned hemiparkinsonian rats.[23]

Although all the MPTP-NIr group achieved better clinical scores (and behavioral activity) than the MPTP group, some achieved much better scores than others. Whereas some in the MPTP-NIr group displayed moderate clinical signs (MPTP-NIr2), others displayed little, if any, sign of clinical impairment (MPTP-NIr1). In contrast to these variations, each monkey of the MPTP group, without exception, developed severe clinical signs, and no distinct subgroups were distinguished. Hence, the efficacy of the NIr application, rather than the MPTP dose regime(s), was the likely contributing factor to the development of these different MPTP-NIr subgroups. Following this thinking, the reason we had 2 clear MPTP-NIr subgroups may be related to the presence of hematic fluid in the optical fibers in 1 of the subgroups (MPTP-NIr2). Hemoglobin has been reported to absorb NIr, certainly when in the 670nm range,[42] and hence may have reduced the effectiveness of NIr, leading to an increase in the clinical scores in this MPTP-NIr subgroup. Future studies may explore this issue further, namely the absorption of NIr by blood and subsequent reduction in NIr efficacy, together with how to minimize hemorrhage infiltration during the assembly of the

implantable device components or during the implantation of the optical fibers.

The reduced clinical signs in the MPTP-NIr group were still evident well after the period of NIr treatment, up to 3 weeks after in many of the cases (see Fig 1). This indicated that the therapeutic effects of NIr (ie, the mitochondrial and other cellular benefits; see below) were rather long-lasting and not confined to periods when NIr was being applied. This key finding suggests that, in the subacute MPTP model we used, NIr mitigated the toxicity of MPTP and that this was maintained for periods well beyond both the administration of MPTP and the end of NIr treatment. This would negate the use of continuous NIr treatment in this animal model, where the toxic insult is not likely to recur. By contrast, in parkinsonian patients—where the degenerative process is ongoing—NIr may well have to be applied on a more regular basis, perhaps once or twice per day.

No Sign of Toxicity in the Brain by NIr

There was no evidence of tissue toxicity by NIr.[13,42–44] Our histological sections and MRI scans revealed no signs of a major inflammatory response or necrosis caused by NIr, particularly in the midline midbrain where the NIr was most intense, and there were no differences in the sizes of sham and NIr-treated implant sites. The only tissue damage observed was mechanical, being caused by the surgical implantation of the optical fiber itself. In both sham and NIr-treated cases, similar patterns of tissue displacement and gliosis were evident along the entire course of the optical fiber tract through the forebrain and near the implant site in the midbrain. Finally, if the NIr was toxic to tissue, one would have expected negative behavioral outcomes and morbidity, particularly after treatment to the midline midbrain, a region that includes, and/or is very near, centers that control critical life functions.[45] This was clearly not the case in the MPTP-NIr group, with their behavior being much improved compared to the MPTP group.

Evidence for Neuroprotection by NIr

There have been a number of previous studies reporting neuroprotection, a slowing or stopping of cell death, by a range of different agents in several rodent models of PD. Unfortunately, such evidence has not been as forthcoming in PD patients.[4–7] One of the reasons contributing to this lack of success has been the paucity of testing neuroprotective agents in nonhuman primate models of PD,[29–31,46] where the cell-to-cell interactions are likely to be more complex than in rodents and similar to humans. The testing of neuroprotective agents in nonhuman primates is considered the final key step before clinical trial,[5] and the monkey MPTP model is the best available currently for PD.[4–7]

In this study, we provided evidence for neuroprotection in a nonhuman primate model of PD, confirming previous studies on rodent models of the disease.[17–25] The MPTP-NIr1 group, the group that had few clinical signs, had a preservation of nigral Nissl-stained (~20%) and TH^+ (~40%) cells and striatal TH^+ terminals (~60%). Hence, the NIr in these cases saved not only the cells themselves (true neuroprotection), but also their functional phenotype (functional neuroprotection). In addition, the MPTP-NIr2 group, the group that had moderate clinical signs, showed evidence for neuroprotection, with a preservation of nigral TH^+ cells. As with our behavioral analysis, this more limited neuroprotection in the MPTP-NIr2 group may be related to the presence of hematic fluid in the optical fiber limiting NIr exposure of the SNc (see above).

Does the Neuroprotection Underlie Reductions in Clinical Signs?

The reduction in clinical impairment in the MPTP-NIr group is likely to be due to neuroprotection. NIr has been shown to stimulate mitochondrial activity, increasing ATP content and electron transfer in the respiratory chain through activation of photoacceptors (eg, cytochrome oxidase), together with influencing reactive oxygen species and the induction of various transcription factors.[11–13,42,43] NIr presumably induced such factors to neuroprotect dopaminergic cells against MPTP insult, thereby preserving their functional capacity for dopaminergic transmission through the striatum and basal ganglia.[39–41] This preservation would have, in turn, generated the reduction in clinical signs evident in the NIr-treated animals. We found that the monkeys with minimal clinical impairment (MPTP-NIr1) had more surviving dopaminergic cells and terminations than the monkeys with either moderate (MPTP-NIr2) or in particular severe (MPTP) clinical impairment. As a consequence, we found a good correlation between the extent of nigral and striatal lesion and peak clinical score in individual monkeys in these groups (see Fig 8).

Although there were generally more cells and fewer clinical signs in the MPTP-NIr groups than in the MPTP group, they never quite reached control levels. In particular, the density of striatal terminals was affected heavily by MPTP insult and NIr treatment offered only limited protection to these terminations (see Figs 6C, 7C, F, I). Nevertheless, what was preserved in the striatum after NIr treatment appeared sufficient to reduce clinical impairment, particularly in the MPTP-NIr1 group. Our finding that there was a preservation of

functional phenotype (ie, TH) in nigral cells of both the MPTP-NIr1 and MPTP-NIr2 groups provides further encouragement; these surviving TH^+ cells may well sprout axons and re-form synaptic connectivity in the striatum,[35] perhaps leading to a further reduction in clinical signs at a later stage. It will be the challenge of future endeavors to reveal precisely how NIr neuroprotects cells and how it impacts on dopaminergic transmission through the basal ganglia.

Conclusions

Within the limitations of the subacute MPTP primate model of PD,[29,30,33] we have results that are highly applicable to humans. Although our model does not mimic faithfully the progressive nature of the disease, of particular relevance is our central finding that, during a period when MPTP insult generated severe clinical signs and considerable cell loss, NIr offset these signs and reduced the cell loss. These are features that characterize few agents in primate models of disease and ones that provide encouragement that NIr could be an effective therapeutic agent in patients. Overall, our results contribute to the basic science proof-of-concept template in a nonhuman primate model of PD, one necessary for translation to clinical trial.

Acknowledgment

This study was funded by the Michael J. Fox Foundation, Credit Agricole Sud Rhones Alpes, Edmond J. Safra Philanthropic Foundation, France Parkinson and French National Research Agency (ANR Carnot Institute), Tenix Corporation, and Salteri family. D.M.J. is an Early Career Fellow of the National Health and Medical Research Council Australia. J.S. was supported by the Sir Zelman Cowen Universities Fund.

We thank S. Spana, G. Barboux, C. Perrin, C. Zenga, and M. D'Orchymont for excellent technical assistance; B. Webster for comments on an early version of the manuscript; and Boston Scientific for providing free implantable items as well as providing a major technological effort in adapting the spectra stimulators for the special needs of powering the laser sources.

Author Contributions

C.M., C.C., N.T., J.M., and A.-L.B. were involved in concept and study design. All authors were involved in data acquisition and analysis. J.M., A.-L.B., C.M., J.S., and D.M.J. were involved in drafting the manuscript and figures. All authors edited and approved the final version of the manuscript. F.D. and C.M. are joint first authors.

Potential Conflicts of Interest

C.M., D.A.: grants/grants pending, Fondation France Parkinson. N.T.: travel expenses, AB Medica, Sociedad Latinoamericana Neurocirugia Funcional.

References

1. Blandini F, Nappi G, Tassorelli C, Martignoni E. Functional changes of the basal ganglia circuitry in Parkinson's disease. Prog Neurobiol 2000;62:63–88.
2. Bergman H, Deuschl G. Pathophysiology of Parkinson's disease: from clinical neurology to basic neuroscience and back. Mov Disord 2002;17(suppl 3):S28–S40.
3. Jankovic J. Parkinson's disease: clinical features and diagnosis. J Neurol Neurosurg Psychiatr 2008;79:368–376.
4. Olanow CW, Kieburtz K, Schapira AHV. Why have we failed to achieve neuroprotection in Parkinson's disease? Ann Neurol 2008; 64(suppl 2):S101–S110.
5. Bezard E, Yue Z, Kirik D, Spillantini MG. Animal models of Parkinson's disease: limits and relevance to neuroprotection studies. Mov Disord 2013;28:61–70.
6. Jankovic J, Poewe W. Therapies in Parkinson's disease. Curr Opin Neurol 2012;25:433–447.
7. Schapira AHV, Olanow CW, Greenamyre JT, Bezard E. Slowing of neurodegeneration in Parkinson's disease and Huntington's disease: future therapeutic perspectives. Lancet 2014;384:545–555.
8. Rinne JO. Nigral degeneration in Parkinson's disease. Mov Disord 1993;8(suppl 1):S31–S35.
9. Benabid AL, Pollak P, Gross C, et al. Acute and long-term effects of subthalamic nucleus stimulation in Parkinson's disease. Stereotact Funct Neurosurg 1994;62:76–84.
10. Krack P, Batir A, Van Blercom N, et al. Five-year follow-up of bilateral stimulation of the subthalamic nucleus in advanced Parkinson's disease. N Engl J Med 2003;349:1925–1934.
11. DeSmet K, Buchmann E, Henry M, et al. Near-infrared light as a possible treatment option for Parkinson's disease and laser eye injury. Proc SPIE Int Soc Opt Eng 2009;716503–716503-10.
12. Quirk BJ, Desmet KD, Henry M, et al. Therapeutic effect of near infrared (NIR) light on Parkinson's disease models. Front Biosci 2012;4:818–823.
13. Johnstone D, Coleman K, Moro C, et al. The potential of light therapy in Parkinson's disease. Chronophysiol Ther 2014;4:1–14.
14. Liang HL, Whelan HT, Eells JT, Wong-Riley MTT. Near-infrared light via light-emitting diode treatment is therapeutic against rotenone- and 1-methyl-4-phenylpyridinium ion-induced neurotoxicity. Neuroscience 2008;153:963–974.
15. Ying R, Liang HL, Whelan HT, et al. Pretreatment with near-infrared light via light-emitting diode provides added benefit against rotenone- and MPP+-induced neurotoxicity. Brain Res 2008;1243:167–173.
16. Trimmer PA, Schwartz KM, Borland MK, et al. Reduced axonal transport in Parkinson's disease cybrid neurites is restored by light therapy. Mol Neurodegener 2009;4:26.
17. Shaw VE, Spana S, Ashkan K, et al. Neuroprotection of midbrain dopaminergic cells in MPTP-treated mice after near-infrared light treatment. J Comp Neurol 2010;518:25–40.
18. Peoples C, Spana S, Ashkan K, et al. Photobiomodulation enhances nigral dopaminergic cell survival in a chronic MPTP mouse model of Parkinson's disease. Parkinsonism Relat Disord 2012;18: 469–476.

19. Moro C, El Massri N, Torres N, et al. Photobiomodulation inside the brain: a novel method of applying near-infrared light intracranially and its impact on dopaminergic cell survival in MPTP-treated mice. J Neurosurg 2014;120:670–683.
20. Moro C, Torres N, El Massri N, et al. Photobiomodulation preserves behaviour and midbrain dopaminergic cells from MPTP toxicity: evidence from two mouse strains. BMC Neurosci 2013;14:40.
21. Johnstone DM, El Massri N, Moro C, et al. Indirect application of near infrared light induces neuroprotection in a mouse model of parkinsonism—an abscopal neuroprotective effect. Neuroscience 2014;274:93–101.
22. Reinhart F, Massri NE, Darlot F, et al. 810nm near-infrared light offers neuroprotection and improves locomotor activity in MPTP-treated mice. Neurosci Res 2015;92:86–90.
23. Reinhart F, El Massri N, Darlot F, et al. Evidence for improved behaviour and neuroprotection after intracranial application of near infrared light in a hemi-parkinsonian rat model. J Neurosurg (in press).
24. El Massri N, Johnstone DM, Peoples CL, et al. The effect of different doses of near infrared light on dopaminergic cell survival and gliosis in MPTP-treated mice. Int J Neurosci (in press) PMID: 25469453.
25. Purushothuman S, Nandasena C, Johnstone DM, et al. The impact of near-infrared light on dopaminergic cell survival in a transgenic mouse model of parkinsonism. Brain Res 2013;1535:61–70.
26. Shaw VE, Peoples C, Spana S, et al. Patterns of Cell Activity in the subthalamic region associated with the neuroprotective action of near-infrared light treatment in MPTP-treated mice. Parkinsons Dis 2012;2012:296875.
27. Whelan HT, DeSmet KD, Buchmann EV, et al. Harnessing the cell's own ability to repair and prevent neurodegenerative disease. SPIE Newsroom 2008;24:1–3.
28. Torres N, Chabardes S, Piallat B, et al. Body fat and body weight reduction following hypothalamic deep brain stimulation in monkeys: an intraventricular approach. Int J Obes (Lond) 2012;36:1537–1544.
29. Wallace BA, Ashkan K, Heise CE, et al. Survival of midbrain dopaminergic cells after lesion or deep brain stimulation of the subthalamic nucleus in MPTP-treated monkeys. Brain 2007;130(pt 8):2129–2145.
30. Benazzouz A, Boraud T, Dubédat P, et al. Riluzole prevents MPTP-induced parkinsonism in the rhesus monkey: a pilot study. Eur J Pharmacol 1995;284:299–307.
31. Bezard E, Gerlach I, Moratalla R, et al. 5-HT1A receptor agonist-mediated protection from MPTP toxicity in mouse and macaque models of Parkinson's disease. Neurobiol Dis 2006;23:77–86.
32. Bezard E, Dovero S, Prunier C, et al. Relationship between the appearance of symptoms and the level of nigrostriatal degeneration in a progressive 1-methyl-4-phenyl-1,2,3,6-tetrahydropyridine-lesioned macaque model of Parkinson's disease. J Neurosci 2001;21:6853–6861.
33. Ashkan K, Wallace BA, Mitrofanis J, et al. SPECT imaging, immunohistochemical and behavioural correlations in the primate models of Parkinson's disease. Parkinsonism Relat Disord 2007;13:266–275.
34. Schneider JS, Gonczi H, Decamp E. Development of levodopa-induced dyskinesias in parkinsonian monkeys may depend upon rate of symptom onset and/or duration of symptoms. Brain Res 2003;990:38–44.
35. Porras G, Li Q, Bezard E. Modeling Parkinson's disease in primates: the MPTP model. Cold Spring Harb Perspect Med 2012;2:a009308.
36. Frey S, Pandya DN, Chakravarty MM, et al. An MRI based average macaque monkey stereotaxic atlas and space (MNI monkey space). Neuroimage 2011;55:1435–1442.
37. Yushkevich PA, Piven J, Hazlett HC, et al. User-guided 3D active contour segmentation of anatomical structures: significantly improved efficiency and reliability. Neuroimage 2006;31:1116–1128.
38. Yaroslavsky AN, Schulze PC, Yaroslavsky IV, et al. Optical properties of selected native and coagulated human brain tissues in vitro in the visible and near infrared spectral range. Phys Med Biol 2002;47:2059.
39. Javoy-Agid F, Hirsch EC, Dumas S, et al. Decreased tyrosine hydroxylase messenger RNA in the surviving dopamine neurons of the substantia nigra in Parkinson's disease: an in situ hybridization study. Neuroscience 1990;38:245–253.
40. Jackson-Lewis V, Jakowec M, Burke RE, Przedborski S. Time course and morphology of dopaminergic neuronal death caused by the neurotoxin 1-methyl-4-phenyl-1,2,3,6-tetrahydropyridine. Neurodegeneration 1995;4:257–269
41. Björklund A, Rosenblad C, Winkler C, Kirik D. Studies on neuroprotective and regenerative effects of GDNF in a partial lesion model of Parkinson's disease. Neurobiol Dis 1997;4:186–200.
42. Chung H, Dai T, Sharma SK, et al. The nuts and bolts of low-level laser (light) therapy. Ann Biomed Eng 2012;40:516–533.
43. Rojas J, Gonzaalez-Lima F. Low-level light therapy of the eye and brain. Eye Brain 2011;3:49–67.
44. McCarthy TJ, De Taboada L, Hildebrandt PK, et al. Long-term safety of single and multiple infrared transcranial laser treatments in Sprague-Dawley rats. Photomed Laser Surg 2010;28:663–667.
45. Waraczynski M, Perkins M, Acheson A. Lesions of midline midbrain structures leave medial forebrain bundle self-stimulation intact. Behav Brain Res 1999;103:175–184.
46. Oiwa Y, Nakai K, Itakura T. Histological effects of intraputaminal infusion of glial cell line-derived neurotrophic factor in Parkinson disease model macaque monkeys. Neurol Med Chir (Tokyo) 2006;46:267–275; discussion 275–276.
47. Paxinos G, Huang X, Toga A. The Rhesus monkey brain in stereotaxic coordinates. San Diego, CA: Academic Press, 1999.